

Comparison of the accuracy of ^{99m}Tc -3P₄-RGD₂ SPECT and CT in diagnosing solitary pulmonary nodules

HAISHAN ZHANG¹, SHI GAO¹, BIN CHEN¹ and GUANGHUI CHENG²

Departments of ¹Nuclear Medicine and ²Radiotherapy, China-Japan Union Hospital, Jilin University, Changchun, Jilin 130033, P.R. China

Received December 2, 2014; Accepted January 19, 2016

DOI: 10.3892/ol.2016.5030

Abstract. The aim of the present study was to compare technetium-99m-(polyethylene glycol-4)₃-(Arg-Gly-Asp)₂ (^{99m}Tc -3P₄-RGD₂) single-photon emission computed tomography (SPECT) and computed tomography (CT) in the noninvasive differentiation of solitary pulmonary nodules (SPNs). The present study prospectively investigated a consecutive series of 24 patients with SPN, who were newly diagnosed using radiography between September 2012 and January 2014. All patients underwent ^{99m}Tc -3P₄-RGD₂ SPECT and CT scans using a dual-head variable-angle γ -camera equipped with high-resolution collimators. A blinded panel of two thoracic radiologists for CT and three nuclear physicians for SPECT analyzed the images using a 5-grade scale. The SPECT images were also semi-quantitatively evaluated using tumor to non-tumor localization ratios (T/NT). The results were verified by pathological examination of the biopsy material obtained from each patient with SPN, and receiver operating characteristic (ROC) curves were generated from these results. The present results revealed that there were 17 malignant and 7 benign SPNs among the 24 patients with SPN. The mean size of the SPN was 2.1±0.6 cm. Sensitivity of visual analysis for SPECT and CT were 100.0 and 82.4%, respectively, and specificity was 71.4% for the two methods. When the T/NT SPECT semiquantitative analysis (ratio, 1.64) was used as a cut-off, the sensitivity and specificity of SPECT were 100.0 and 71.4%, respectively. The areas under the ROC curves were 0.840 for visual analysis of SPECT [95% confidence interval (CI), 0.600-1.000], 0.849 for semiquantitative analysis of SPECT (95% CI, 0.618-1.000) and 0.815 for CT (95% CI, 0.626-1.000). In conclusion, the present results suggest that ^{99m}Tc -3P₄-RGD₂ SPECT is more accurate than CT in the detection of malignant SPN, and visual analysis appears to be sufficient for the characterization of SPN.

Introduction

Lung cancer continues to be a major public health concern in the USA and other Western countries (1). In 2015, the American Cancer Society reported that 221,200 novel cases of lung cancer were diagnosed in the USA, accounting for ~13% of all cancer diagnoses, and 27% of all cancer-associated mortalities in the USA (2).

A strategy for the reduction of lung cancer-associated mortality rates is to diagnose the disease while it is at an early stage (3). A solitary pulmonary nodule (SPN) is defined as a single lesion in the lung completely surrounded by lung parenchyma with a diameter <3 cm, which is observed on chest radiography and is often the first identifiable manifestation of lung carcinoma (4,5). Previous studies have demonstrated that 68-75% of SPNs are malignant (6,7). Timely and efficient assessment of these nodules is critical for improved patient management (8).

In the USA, >150,000 novel SPNs are identified each year using conventional chest radiography (9). Numerous pulmonary nodules are detected annually using chest computed tomography (CT), since this technique is becoming more widely used in USA patient populations (10). However, CT has limited diagnostic accuracy, since the interpretation of the images relies principally on the size of the lesion and other non-specific findings (11). Magnetic resonance imaging is not a routine examination for the diagnosis of SPN, due to known artefacts that result from tissue-air interfaces and relatively low spatial resolution (12,13). Contrast-enhanced ultrasonography may be used to diagnose pulmonary nodules, but it does not provide a complete image of the lungs due to a variety of reasons, including the lungs being full of gas and interference from the osseous thorax (14). Thus, traditional anatomic imaging does not characterize if the SPN is malignant or benign, which leads to numerous unnecessary surgical lung biopsies (15). Therefore, novel imaging modalities are required to reduce the number of excisional lung biopsies for the diagnosis of SPN.

Fluorine-18-fluorodeoxyglucose (^{18}F -FDG) positron emission tomography (PET) is considered to be the most effective method in the differential diagnosis of indeterminate SPN, but its use is limited due to the high cost of the equipment and lack of availability, particularly in developing countries (16). By contrast, single-photon emission

Correspondence to: Professor Guanghui Cheng, Department of Radiotherapy, China-Japan Union Hospital, Jilin University, 126 Xiantai Street, Changchun, Jilin 130033, P.R. China
E-mail: chengguanghui549@126.com

Key words: ^{99m}Tc -3P₄-RGD₂, SPECT/CT, solitary pulmonary nodule

computed tomography (SPECT) is more widely used, since it has a lower cost (17). Radioactive tracers for SPECT, including technetium-99m (^{99m}Tc)-octreotide acetate (18), ^{99m}Tc -depreotide, ^{99m}Tc -methoxyisobutylisonitrile (19) and ^{99m}Tc -tetrofosmin (20), have been employed in the diagnosis of SPN using diagnostic imaging procedures.

Previous studies have been performed using ^{99m}Tc -(polyethylene glycol-4)₃-(Arg-Gly-Asp)₂ (^{99m}Tc -3P₄-RGD₂) as a novel radioactive molecular probe (21-23). This radiopharmaceutical demonstrated a high binding affinity to integrin $\alpha\beta 3$ *in vitro*, and exhibited significantly increased tumor uptake and improved *in vivo* kinetics in animal models (24). In addition, ^{99m}Tc -3P₄-RGD₂ is easily prepared using freeze-dried kits, has a high-labeling yield and radiochemical purity, and does not exhibit adverse events *in vivo* in nonhuman primates (24). Previously, ^{99m}Tc -3P₄-RGD₂ has been used for the noninvasive differentiation of breast neoplasms (21), and the tracer has demonstrated an impressive image quality with a high sensitivity (83%) in detecting breast cancer.

The primary aim of the present study was to evaluate the use of ^{99m}Tc -3P₄-RGD₂ SPECT in patients with SPN. An additional aim was to compare the diagnostic accuracy of visual and semiquantitative indices of SPECT and CT for the noninvasive differentiation of benign versus malignant SPN using receiver operating characteristic (ROC) analysis.

Materials and methods

Patients. The present prospective study consisted of a consecutive series of 24 patients [14 men and 10 women; age range, 18-77 years; mean age \pm standard deviation (SD), 48.79 \pm 15.53 years], who had a SPN diameter between 1 and 3 cm on a CT scan that was performed between September 2012 and January 2014 at the China-Japan Union Hospital, Jilin University (Changchun, China). The diameter of all SPNs were calculated based on the maximum lesion diameter observed on CT scanning performed prior to the enrollment of the patients in the present study, which was assessed by thoracic surgeons and radiologists (Department of Radiology, China-Japan Union Hospital, Jilin University). A definitive diagnosis was achieved using transthoracic fine-needle aspiration biopsy or bronchoscopic biopsy. Patients with a malignant SPN underwent surgical resection. Permission to use a novel radiopharmaceutical was obtained from local independent ethics committees and the Institutional Review Board of China-Japan Union Hospital, Jilin University (Changchun, China). Written informed consent to participate in the present scintimammography study was obtained from all patients.

Radiopharmaceutical. The ^{99m}Tc -3P₄-RGD₂ conjugate was generously provided by the Medical Isotopes Research Center of Peking University (Beijing, China) as a freeze-dried kit. ^{99m}Tc -3P₄-RGD₂ was labeled with Na $^{99m}\text{TcO}_4$ (China Institute of Atomic Energy, Beijing, China) solution, followed by 20-min incubation at 100°C. Quality control was conducted using radioactive thin-layer chromatography (using an AR-2000 radio-TLC Imaging Scanner, Bioscan, Inc., Washington, DC, USA), which enabled to measure a high labeling

yield of ~95%. A molybdenum-technetium generator was provided by Beijing Atom Hi-Tech Co., Ltd. (Beijing, China).

Acquisition of lung SPECT/CT images with ^{99m}Tc -3P₄-RGD₂. ^{99m}Tc -3P₄-RGD₂, with a mean radioactivity of 378 \pm 86 MBq, was administered via a single intravenous bolus injection in the contralateral arm to the affected lung in each patient, followed by a 10 ml saline flush (Sichuan Kelun Pharmaceutical Co., Ltd., Sichuan, China). Acquisition of the images was obtained at 60 min post-injection. During imaging, patients were in supine position with raised arms. The SPECT/CT system (Precedence SPECT/CT System; Philips Healthcare, Andover, MA, USA) consisted of a dual-head variable-angle γ -camera equipped with low-energy high-resolution collimators and a multi-slice spiral CT component optimized for rapid rotation. Local X-ray scanning (Precedence SPECT/CT System; Philips Healthcare) was performed to image the region of SPN. The following CT scan was set at a matrix of 256x256 pixels, 130 kV, 17 mAs, B60s kernel and a 5-mm slice thickness. Following the collection of CT images, the detecting bench was positioned automatically for SPECT data collection. The matrix was 128x128 pixels and the photopeak was centered at 140 keV, with a symmetrical 20% window. Imaging was performed using 6° angular steps in a 20-sec time frame. The distance between the chest and the detector was minimized as much as possible. Digital Imaging and Communications in Medicine image files of each patient were saved on optic disks (Philips Healthcare) and transferred to Extended Brilliance Workspace 4.5 (Philips Healthcare) for centralized reconstruction, reading and analysis. A fusion SPECT and CT image was produced using Syntegra software (Philips Medical Systems B.V., Eindhoven, The Netherlands).

Evaluation criteria. Three experienced nuclear physicians (Department of Nuclear Medicine, China-Japan Union Hospital, Jilin University) who were blinded to the patients clinical information, physical examinations and radiological findings interpreted the ^{99m}Tc -3P₄-RGD₂ scans individually. The following qualitative interpretation grades were used: Grade 1, no uptake; grade 2, uptake lower than mediastinum; grade 3, uptake equivalent to mediastinum; grade 4, uptake between mediastinum and liver; and grade 5, uptake higher than liver. For semiquantitative analysis, a region of interest was drawn around the entire nodule to the contralateral normal lung tissue. Tumor to non-tumor localization ratios (T/NT) were determined. In the case of grade 1, the T/NT was considered to be 1, due to the absence of uptake. The results were reached by a consensus of the three nuclear physicians.

The CT images were evaluated by two experienced thoracic radiologists who were blinded to the clinical data of the patients. In visual analysis, the image quality of the SPN, including size, shape, conspicuity, margin and presence of calcification, were evaluated. Five diagnostic groups were defined to describe the possible malignancy of each nodule: 1, definitely benign; 2, possibly benign; 3, indeterminate; 4, possibly malignant; and 5, definitely malignant.

Statistical analysis. All numerical results were reported as the mean \pm SD. The statistical differences of the T/NT values between patients with malignant and benign nodules

Table I. Characteristics of 24 patients with malignant and benign solitary pulmonary nodules.

Patient no.	Pathology	Gender	Age, years	Nodule size, cm	T/NT	SPECT grade	CT grade
1	Squamous cell carcinoma	Female	38	1.6	2.27	4	3
2	Squamous cell carcinoma	Female	27	3.0	3.28	5	5
3	Squamous cell carcinoma	Male	18	2.5	1.87	3	2
4	Squamous cell carcinoma	Female	77	1.9	2.64	4	2
5	Squamous cell carcinoma	Female	39	2.0	2.56	3	3
6	Squamous cell carcinoma	Female	48	1.7	3.05	4	4
7	Squamous cell carcinoma	Male	43	2.8	2.18	3	5
8	Small cell carcinoma	Male	58	2.9	2.95	3	4
9	Small cell carcinoma	Male	48	2.3	2.93	5	4
10	Small cell carcinoma	Male	67	2.2	2.18	3	5
11	Small cell carcinoma	Male	48	2.1	2.22	4	2
12	Adenocarcinoma	Female	57	2.9	2.07	3	4
13	Adenocarcinoma	Female	54	3.0	2.41	4	3
14	Adenocarcinoma	Male	32	1.1	3.27	5	4
15	Adenocarcinoma	Male	52	1.9	2.87	4	5
16	Adenocarcinoma	Male	68	2.7	2.38	4	3
17	Adenocarcinoma	Male	54	1.4	2.77	3	3
18	Tuberculoma	Male	37	1.4	1.04	1	2
19	Tuberculoma	Male	26	2.2	1.41	3	2
20	Tuberculoma	Female	51	2.1	2.18	1	3
21	Tuberculoma	Female	52	2.4	1.10	1	2
22	Inflammatory pseudotumor	Female	67	1.1	3.24	5	4
23	Reactive hyperplasia of lymph node	Male	35	2.3	1.19	1	2
24	Hamartoma	Male	75	1.2	1.06	1	1

Solitary pulmonary nodules were detected using transthoracic fine-needle aspiration biopsy or bronchoscopic biopsy. T/NT, tumor to non-tumor localization ratio; SPECT, single-photon emission computed tomography; CT, computed tomography.

were assessed using Student's *t* test. T/NT values were also compared across the various histological types of lung carcinoma. MedCalc software 12.7.7 (MedCalc Software bvba, Ostend, Belgium) was used to determine the optimal visual interpretation grade of SPECT and CT and the cut-off values of semiquantitative indices of SPECT for the detection of SPN. Linear regression analysis was performed to determine the powerful variables for the prediction of SPN. The incremental diagnostic value of semiquantitative indice analysis was performed using the area under the curve in ROC analysis. $P < 0.05$ was considered to indicate a statistically significant difference.

Results

Patients characteristics. Samples for histological examination were obtained using transthoracic fine-needle aspiration biopsy in 18 patients and bronchoscopy biopsy in 6 patients. In total, 17 out of 24 (71%) SPNs were malignant and 7 (29%) were benign. Among the malignant etiologies, 7 patients had squamous cell carcinoma, 6 adenocarcinoma and 4 small cell carcinoma. The benign aetiologies consisted of 4 tuberculomas, 1 inflammatory pseudotumor, 1 hamartoma and

1 reactive hyperplasia of lymph node. The characteristics of the 24 patients are detailed in Table I.

T/NT. In all patients with SPN, the mean T/NT value \pm SD was 2.20 ± 0.72 (range, 1.04–3.28). In patients with malignant SPNs, the mean T/NT value \pm SD was 2.58 ± 0.43 (range, 1.87–3.28), and in patients with benign SPNs it was 1.60 ± 0.83 (range, 1.04–3.24) ($P = 0.059$). The semiquantitative analysis demonstrated a higher T/NT ratio in malignant lesions compared with benign lesions, although this was not statistically significant. Furthermore, the mean nodule size for malignant and benign SPN was 2.24 ± 0.59 cm, and there was no significant correlation between the T/NT value and the size of the nodule ($P = 0.92$). The various histological types of primary lung carcinoma did not affect the SPECT results [T/NT ratios (Table I): Squamous cell carcinoma, 2.55 ± 0.49 ; adenocarcinoma, 2.63 ± 0.43 ; and small cell lung carcinoma, 2.57 ± 0.43]. Representative examples of a high focal uptake in carcinomas are presented in Fig. 1.

Optimal cut-off values. The optimal cut-off values for CT interpretation, SPECT visual analysis and semiquantitative analysis were visual score = 3, visual score = 2 and T/NT = 1.64, respectively. The sensitivity, specificity, accuracy, positive predictive

Table II. Diagnostic test parameters of three diagnostic methods for the characterization of solitary pulmonary nodules.

Parameters	CT interpretation	Visual analysis of SPECT	Semiquantitative analysis of SPECT
Accuracy, % (95% CI)	79.2 (59.5-90.8)	91.7 (74.2-97.7)	91.7 (74.2-97.7)
Sensitivity, % (95% CI)	82.4 (59.0-93.8)	100.0 (81.6-100.0)	100.0 (81.6-100.0)
Specificity, % (95% CI)	71.4 (35.9-91.8)	71.4 (35.9-91.8)	71.4 (35.9-91.8)
PPV, % (95% CI)	87.5 (64.0-96.5)	89.5 (68.6-97.1)	89.5 (68.6-97.1)
NPV, % (95% CI)	62.5 (30.6-86.3)	100.0 (56.6-100.0)	100.0 (56.6-100.0)

CT, computed tomography; SPECT, single-photon computed emission tomography; CI, confidence interval; PPV, positive predictive value; NPV, negative predictive value.

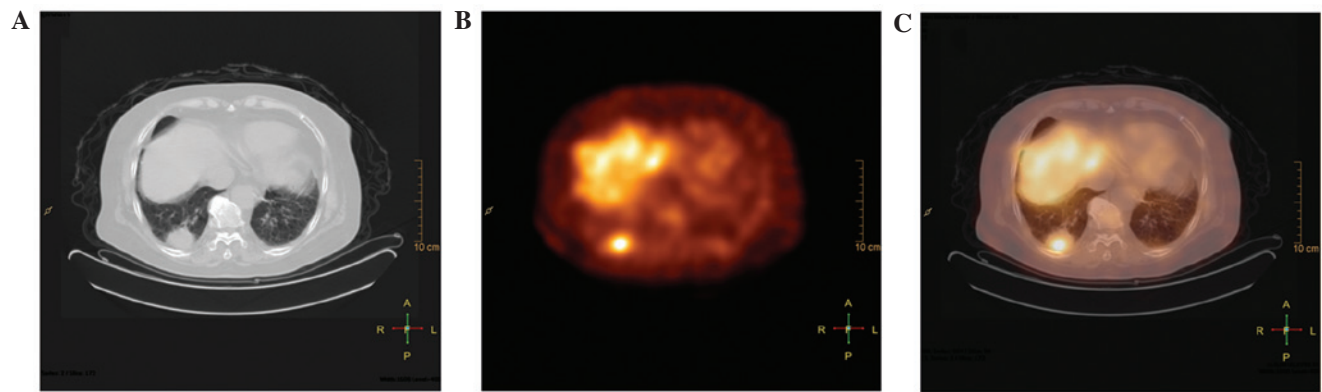


Figure 1. True-positive results for ^{99m}Tc-3P₄-RGD₂ SPECT and SPECT/CT scans, in contrast to a false-positive result for CT. (A) CT, (B) SPECT and (C) CT/SPECT fusion images of a 68 year-old man (patient no. 16) with a 2.7-cm adenocarcinoma and focal uptake of ^{99m}Tc-3P₄-RGD₂ at the inferior lobe of the right lung (tumor to non-tumor localization ratio, 2.38). ^{99m}Tc-3P₄-RGD₂, technetium-99m-(polyethylene glycol-4)₃-(Arg-Gly-Asp)₂; SPECT, single-photon emission computed tomography; CT, computed tomography.

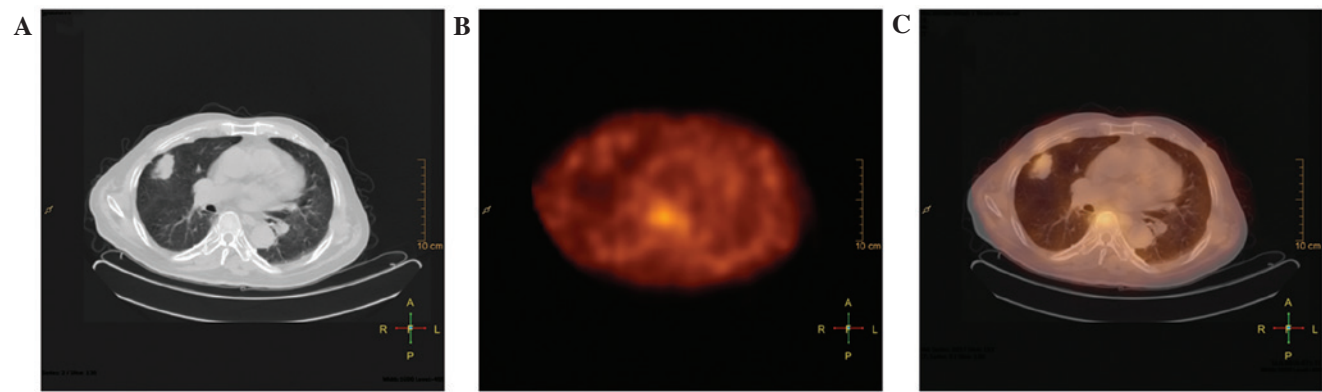


Figure 2. True-negative results for ^{99m}Tc-3P₄-RGD₂ SPECT and SPECT/CT scans, in contrast to a false-negative result for CT. (A) CT, (B) SPECT and (C) CT/SPECT fusion images of a 52 year-old woman (patient no. 21) with a 2.4-cm tuberculoma and low uptake of ^{99m}Tc-3P₄-RGD₂ in the tumor at the middle lobe of the right lung (tumor to non-tumor localization ratio, 1.10). ^{99m}Tc-3P₄-RGD₂, technetium-99m-(polyethylene glycol-4)₃-(Arg-Gly-Asp)₂; SPECT, single-photon emission computed tomography; CT, computed tomography.

value and negative predictive value of the three diagnostic analyses are indicated in Table II.

Visual analysis. The CT scan resulted in 2 false-positive findings (1 tuberculoma and 1 inflammatory pseudotumor) and 3 false-negative findings (2 squamous cell carcinoma and 1 small cell carcinoma) (Fig. 1). Although SPECT visual and semiquantitative analyses also yielded 2 false-positive findings (1 tuberculoma in a different patient and 1 inflammatory

pseudotumor in patient 22), it resulted in no false-negative findings (Fig. 2).

ROC analysis. The empirical ROC areas, which estimated overall diagnostic performance, did not differ significantly among the three diagnostic methodologies (Fig. 3): Semiquantitative analysis of SPECT, 0.849 [95% confidence interval (CI), 0.618-1.000]; visual analysis of SPECT, 0.840 (95% CI, 0.600-1.000); CT interpretation, 0.815 (95% CI,

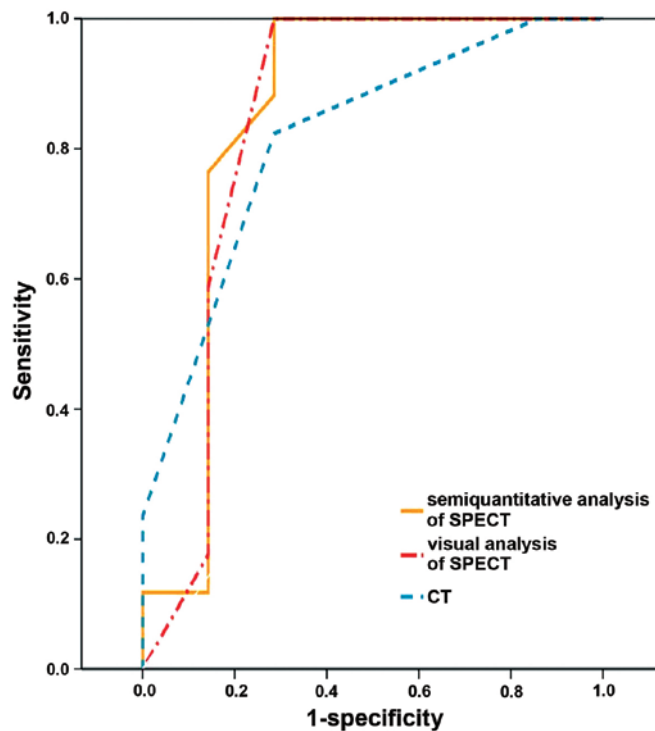


Figure 3. Comparison between CT, visual and semiquantitative analyses of technetium-99m-(polyethylene glycol-4)₃-(Arg-Gly-Asp)₂ single-photon emission CT in the differential diagnosis of malignant and benign solitary pulmonary nodules using receiver operating characteristic analysis. CT, computed tomography; SPECT, single-photon emission computed tomography.

0.626-1.000); semiquantitative analysis of SPECT vs. visual analysis of SPECT ($P=0.521$); semiquantitative analysis of SPECT vs. CT interpretation ($P=0.588$); and visual analysis of SPECT vs. CT interpretation ($P=0.564$).

Discussion

^{99m}Tc-3P₄-RGD₂ is a well-designed, dimeric RGD peptide that exhibits increased uptake in mouse cancer xenografts using scintigraphy (25). The uptake of the RGD-containing peptide, quantified by *in vitro* and *in vivo* studies, has been observed to be proportional to integrin density and tumor size (26-29). In previous studies, the present authors group applied this novel tracer for the noninvasive differentiation of palpable and nonpalpable breast lesions (21), and the tracer demonstrated an impressive image quality with a high sensitivity in detecting breast cancer.

Chest CT, as a conventional imaging method, continues to be important in the evaluation of patients with SPN (30). Radiological findings that suggest SPN malignancy are thickness of the cavity wall and the presence of a speculated or nodular edge, whereas central, laminated or diffuse calcifications are more likely to be associated with a benign etiology (31). However, despite the advances in anatomic and morphological imaging, numerous nodules remain indeterminate, due to the various criteria employed for their characterization as benign or malignant nodules (7). Invasive and expensive diagnostic procedures, including bronchoscopy and surgical exploration, are often undertaken to obtain a specific SPN diagnosis (32). The observation that 60% of removed nodules are benign lesions indicates the requirement for a simple, efficient and non

invasive approach for the differentiation of benign versus malignant nodules (33).

The present study performed a comparison of ^{99m}Tc-3P₄-RGD₂ SPECT and CT for evaluating SPN. The sensitivity of ^{99m}Tc-3P₄-RGD₂ SPECT was superior to that of CT in the present study; however, the difference in performance of the diagnostic methods was not statistically significant. In total, 17.6% of the nodules were characterized as malignant nodules using ^{99m}Tc-3P₄-RGD₂ SPECT. In addition, 5 SPNs were classified as indeterminate using CT, but were correctly diagnosed using ^{99m}Tc-3P₄-RGD₂ SPECT. Visual analysis yielded the same result as semiquantitative analysis for ^{99m}Tc-3P₄-RGD₂ SPECT, indicating that visual analysis may be sufficient for the characterization of SPN.

When grade 2 was used as a cut-off point for visual analysis, SPECT revealed that all malignant SPNs exhibited focal ^{99m}Tc-3P₄-RGD₂ accumulation with varying intensities. However, the negative predictive value of 100% was possibly due to the low number of SPNs characterized ($n=7$). Thus, an additional study with a larger patient population is required to determine the correct negative predictive value. The sensitivity reported in the present study for ^{99m}Tc-3P₄-RGD₂ SPECT is comparable to that of ¹⁸F-FDG PET/CT (83-100%) (34,35). This high sensitivity may be explained by a high prevalence of malignant tumors in the present cohort. Furthermore, the low ^{99m}Tc-3P₄-RGD₂ uptake in the thoracic region also exhibited a high sensitivity for the detection of malignant nodules. Previous studies have recommended targeting ^{99m}Tc-3P₄-RGD₂ to regions of angiogenesis during tumor development, since a tumor size of 0.2-0.3 cm may exhibit angiogenesis (36). Hypothetically, a pharmaceutical with enough binding affinity such as ^{99m}Tc-3P₄-RGD₂ may detect

the majority of tumors with a diameter >1 cm, and may also be the cause of high sensitivity.

In the present study, 1 case of tuberculoma and 1 case of inflammatory pseudotumor exhibited focal ^{99m}Tc -3P₄-RGD₂ uptake. Previous studies have demonstrated that integrin $\alpha\text{v}\beta 3$ is only observed on the luminal surface of endothelial cells during angiogenesis (37); however, angiogenesis is nonspecific in various pathological events (38). By contrast to other benign lesions, inflammation always exhibits a high cell density and vascularity, which are most likely to be responsible for the increased uptake of the tracer (39). Furthermore, integrin $\alpha\text{v}\beta 3$ exists on neutrophils, monocytes and vascular smooth muscle cells (40,41); therefore, also contributing to the false-positive results using ^{99m}Tc -3P₄-RGD₂ SPECT.

In conclusion, the present results suggest that a ^{99m}Tc -3P₄-RGD₂ SPECT scan is the most beneficial method for the detection of malignant SPN, and visual analysis appears to be sufficient for the characterization of SPN.

Acknowledgements

The authors would like to thank the National Natural Science Foundation of China (Beijing, China; grant no. 81271606) and the Research Fund of Science and Technology Department of Jilin Province (Changchun, China; grant no. 20150520154JH) for financially supporting the present study.

References

- Kristiansen C, Schytte T, Hansen KH, Holtved E and Hansen O: Academy of Geriatric Cancer Research (AgeCare): Trends in lung cancer in elderly in Denmark, 1980-2012. *Acta Oncol* 55 (Suppl 1): 46-51, 2016.
- Siegel RL, Miller KD and Jemal A: Cancer statistics, 2015. *CA Cancer J Clin* 65: 5-29, 2015.
- Novaes FT, Cataneo DC, Ruiz Junior RL, Defaveri J, Michelin OC and Cataneo AJ: Lung cancer: Histology, staging, treatment and survival. *J Bras Pneumol* 34: 595-600, 2008.
- Tan BB, Flaherty KR, Kazerooni EA and Iannettoni MD: American College of Chest Physicians: The solitary pulmonary nodule. *Chest* 123 (Suppl 1): 89S-96S, 2003.
- Winer-Muram HT: The solitary pulmonary nodule. *Radiology* 239: 34-49, 2006.
- Gould MK, Sanders GD, Barnett PG, Rydzak CE, Maclean CC, McClellan MB and Owens DK: Cost-effectiveness of alternative management strategies for patients with solitary pulmonary nodules. *Ann Intern Med* 138: 724-735, 2003.
- Schrevels L, Lorent N, Dooms C and Vansteenkiste J: The role of PET scan in diagnosis, staging, and management of non-small cell lung cancer. *Oncologist* 9: 633-643, 2004.
- Spiro SG, Gould MK and Colice GL; American College of Chest Physicians: Initial evaluation of the patient with lung cancer: Symptoms, signs, laboratory tests, and paraneoplastic syndromes: ACCP evidenced-based clinical practice guidelines (2nd edition). *Chest* 132 (Suppl 3): 149S-160S, 2007.
- Ost D, Fein AM and Feinsilver SH: Clinical practice. The solitary pulmonary nodule. *N Engl J Med* 348: 2535-2542, 2003.
- Fujimoto K: Usefulness of contrast-enhanced magnetic resonance imaging for evaluating solitary pulmonary nodules. *Cancer Imaging* 8: 36-44, 2008.
- Webb WR, Gatsonis C, Zerhouni EA, Heelan RT, Glazer GM, Francis IR and McNeil BJ: CT and MR imaging in staging non-small cell bronchogenic carcinoma: Report of the Radiologic Diagnostic Oncology Group. *Radiology* 178: 705-713, 1991.
- Bergin CJ, Glover GH and Pauly JM: Lung parenchyma: Magnetic susceptibility in MR imaging. *Radiology* 180: 845-848, 1991.
- Suga K, Ogasawara N, Okada M, Hara A and Matsunaga N: Potential of noncontrast electrocardiogram-gated half-Fourier fast-spin-echo magnetic resonance imaging to monitor dynamically altered perfusion in regional lung. *Invest Radiol* 37: 615-625, 2002.
- Sartori S, Postorivo S, Vece FD, Ermili F, Tassinari D and Tombesi P: Contrast-enhanced ultrasonography in peripheral lung consolidations: What's its actual role? *World J Radiol* 5: 372-380, 2013.
- van de Luijngaarden AC1, de Rooy JW, de Geus-Oei LF, van der Graaf WT and Oyen WJ: Promises and challenges of positron emission tomography for assessment of sarcoma in daily clinical practice. *Cancer Imaging* 8: S61-S68, 2008.
- Sim YT, Goh YG, Dempsey MF, Han S and Poon FW: PET-CT evaluation of solitary pulmonary nodules: correlation with maximum standardized uptake value and pathology. *Lung* 191: 625-632, 2013.
- MacManus MP, Hicks RJ, Ball DL, Ciavarella F, Binns D, Hogg A, Kalff V, Ware R, Wirth A, Salminen E and McKenzie A: Imaging with F-18 FDG PET is superior to Tl-201 SPECT in the staging of non-small cell lung cancer for radical radiation therapy. *Australas Radiol* 45: 483-490, 2001.
- Wang L, Yin X, Wang F, Gu J, Lu L, Wu Q, Shen B and Li XF: The usefulness of combined diagnostic CT and (99m)Tc-octreotide somatostatin receptor SPECT/CT imaging on pulmonary nodule characterization in patients. *Cancer Biother Radiopharm* 28: 731-736, 2013.
- Schuermans MM, Ellmann A, Bouma H, Diacon AH, Dyckmans K and Bolliger CT: Solitary pulmonary nodule evaluation with 99mTc-methoxy isobutyl isonitrile in a tuberculosis-endemic area. *Eur Respir J* 30: 1090-1095, 2007.
- Spanu A, Schillaci O, Pirina P, Arru A, Madeddu G, Chessa F, Marongiu P, Solinas ME and Madeddu G: 99mTc-tetrofosmin SPECT in solitary pulmonary nodule evaluation. *Oncol Rep* 16: 763-769, 2006.
- Liu L, Song Y, Gao S, Ji T, Zhang H, Ji B, Chen B, Jia B, Wang F, Xu Z and Ma Q: (99m)Tc-3PRGD2 scintimammography in palpable and nonpalpable breast lesions. *Mol Imaging* 13: 1-7, 2014.
- Jin X, Meng Y, Zhu Z, Jing H and Li F: Elevated 99mTc 3PRGD2 activity in benign metastasizing leiomyoma. *Clin Nucl Med* 38: 117-119, 2013.
- Huang C, Zheng Q and Miao W: Study of novel molecular probe 99mTc-3PRGD2 in the diagnosis of rheumatoid arthritis. *Nucl Med Commun* 36: 1208-1214, 2015.
- Jia B, Liu Z, Zhu Z, Shi J, Jin X, Zhao H, Li F, Liu S and Wang F: Blood clearance kinetics, biodistribution, and radiation dosimetry of a kit-formulated integrin $\alpha\text{v}\beta 3$ -selective radiotracer 99mTc-3PRGD 2 in non-human primates. *Mol Imaging Biol* 13: 730-736, 2011.
- Zhou Y, Shao G and Liu S: Monitoring breast tumor lung metastasis by U-SPECT-II/CT with an integrin $\alpha\text{v}\beta 3$ -targeted radiotracer 99mTc-3P-RGD2. *Theranostics* 2: 577-588, 2012.
- Wang L, Shi J, Kim YS, Zhai S, Jia B, Zhao H, Liu Z, Wang F, Chen X and Liu S: Improving tumor-targeting capability and pharmacokinetics of (99m)Tc-labeled cyclic RGD dimers with PEG(4) linkers. *Mol Pharm* 6: 231-245, 2009.
- Zhang X, Xiong Z, Wu Y, Cai W, Tseng JR, Gambhir SS and Chen X: Quantitative PET imaging of tumor integrin $\alpha\text{v}\beta 3$ expression with 18F-FRGD2. *J Nucl Med* 47: 113-121, 2006.
- Liu Z, Jia B, Shi J, Jin X, Zhao H, Li F, Liu S and Wang F: Tumor uptake of the RGD dimeric probe (99m)Tc-G3-2P4-RGD2 is correlated with integrin $\alpha\text{v}\beta 3$ expressed on both tumor cells and neovasculature. *Bioconjug Chem* 21: 548-555, 2010.
- Beer AJ, Haubner R, Sarbia M, Goebel M, Luderschmidt S, Grosu AL, Schnell O, Niemeyer M, Kessler H, Wester HJ, *et al*: Positron emission tomography using [^{18}F]Galacto-RGD identifies the level of integrin $\alpha(v)\beta 3$ expression in man. *Clin Cancer Res* 12: 3942-3949, 2006.
- Wang X, Cao A, Peng M, Hu C, Liu D, Gu T and Liu H: The value of chest CT scan and tumor markers detection in sputum for early diagnosis of peripheral lung cancer. *Zhongguo Fei Ai Za Zhi* 7: 58-63, 2004.
- Maehara Y, Matsumoto M, Matsuura M, Kawasima M, Tateno K and Sakaino K: Pleural thickening associated with solitary pulmonary nodule: Evaluation with thin-slice CT. *Nihon Igaku Hoshasen Gakkai Zasshi* 49: 253-258, 1989 (In Japanese).
- Schwarz C, Schönfeld N, Bittner RC, Mairinger T, Rüssmann H, Bauer TT, Kaiser D and Lodenkemper R: Value of flexible bronchoscopy in the pre-operative work-up of solitary pulmonary nodules. *Eur Respir J* 41: 177-182, 2013.
- Midthun DE: Solitary pulmonary nodule: Time to think small. *Curr Opin Pulm Med* 6: 364-370, 2000.

34. Kim SK, Allen-Auerbach M, Goldin J, Fueger BJ, Dahlbom M, Brown M, Czernin J and Schiepers C: Accuracy of PET/CT in characterization of solitary pulmonary lesions. *J Nucl Med* 48: 214-220, 2007.
35. Jeong SY, Lee KS, Shin KM, Bae YA, Kim BT, Choe BK, Kim TS and Chung MJ: Efficacy of PET/CT in the characterization of solid or partly solid solitary pulmonary nodules. *Lung Cancer* 61: 186-194, 2008.
36. Folkman J: Angiogenesis. *Annu Rev Med* 57: 1-18, 2006.
37. Brooks PC, Clark RA and Cheresh DA: Requirement of vascular integrin $\alpha_v\beta_3$ for angiogenesis. *Science* 264: 569-571, 1994.
38. Mousa SA: α_v Integrin receptors in vascular-mediated disorders. *Med Res Rev* 23: 190-199, 2003.
39. Thurston G, Murphy TJ, Baluk P, Lindsey JR and McDonald DM: Angiogenesis in mice with chronic airway inflammation: Strain-dependent differences. *Am J Pathol* 153: 1099-1112, 1998.
40. Antonov AS, Antonova GN, Munn DH, Mivechi N, Lucas R, Catravas JD and Verin AD: $\alpha_v\beta_3$ integrin regulates macrophage inflammatory responses via PI3 kinase/Akt-dependent NF- κ B activation. *J Cell Physiol* 226: 469-476, 2011.
41. Horton MA: The $\alpha_v\beta_3$ integrin 'vitronectin receptor'. *Int J Biochem Cell Biol* 29: 721-725, 1997.